

Free energy of liquid water on the basis of quasichemical theory and *ab initio* molecular dynamics

D. Asthagiri, Lawrence R. Pratt, and J. D. Kress

Theoretical Division, Los Alamos National Laboratory, Los Alamos, New Mexico 87545, USA

(Received 3 July 2003; published 23 October 2003)

We use *ab initio* molecular dynamics as a basis for quasichemical theory evaluation of the free energy of water near conventional liquid thermodynamic states. The Perdew-Wang-91 (PW91), Perdew-Burke-Ernzerhof (PBE), and revised PBE (rPBE) functionals are employed. The oxygen radial density distribution using the rPBE functional is in reasonable agreement with current experiments, whereas the PW91 and PBE functionals predict a more structured oxygen radial density distribution. The diffusion coefficient with the rPBE functional is in reasonable accord with experiments. Using a maximum entropy procedure, we obtain x_0 from the coordination number distribution x_n for oxygen atoms having n neighbors. Likewise, we obtain p_0 from p_n , the probability of observing cavities of specified radius containing n water molecules. The probability x_0 is a measure of the local chemical interactions and is central to the quasichemical theory of solutions. The probability p_0 , central to the theory of liquids, is a measure of the free energy required to open cavities of defined sizes in the solvent. Using these values and a reasonable model for electrostatic and dispersion effects, the hydration free energy of water in water at 314 K is calculated to be -5.1 kcal/mole with the rPBE functional, in encouraging agreement with the experimental value of -6.1 kcal/mole.

DOI: 10.1103/PhysRevE.68.041505

PACS number(s): 61.25.Em

I. INTRODUCTION

On the basis of its active participation in numerous chemical processes, water should be regarded as an exceptionally chemical liquid. Water is also the most important liquid from the standpoint of understanding life processes; the water molecule is in fact the most important biomolecule. For such reasons, the molecular theory of aqueous solutions is a distinct category of the study of solutions. Higher detail is required for a satisfactory molecular understanding than for nonaqueous solutions, and much of that further molecular detail is unavoidably chemical in nature. Here we report an initial evaluation of the free energy of liquid water using quasichemical theory [1,2] and *ab initio* molecular dynamics (AIMD). In addition to the physical conclusions that can be based upon the observations from the physically motivated quasichemical theory, the present results should also serve as benchmarks for the burgeoning efforts applying AIMD to aqueous solutions.

The extant literature offers several papers on AIMD simulation of water (see Refs. [3–5], and references therein). Some of these simulations, for example, Refs. [3,4], used the Car-Parrinello (CPMD) method, whereas others, for example, Ref. [5] used a Born-Oppenheimer *ab initio* molecular dynamics procedure. Our own past research efforts [6–9] has focused on understanding ion-water systems and chemical reactions in aqueous systems using both the statistical mechanical quasichemical theory of solutions and a Born-Oppenheimer AIMD approach. These works invariably differ in methodological detail but have in common severe limitations of time and length scales that are treated. There is indeed a widespread, undocumented, and perhaps controversial, view that the AIMD calculations typically describe unsatisfactorily “glassy” water at conventional liquid thermodynamic state points. Thus, independent benchmark ef-

forts should be zealously encouraged.

In all of the early AIMD works that considered pure water, the questions have largely centered on understanding the structure and bonding in liquid water (for example, Refs. [3–5]). Quantities often considered are the radial density distribution and the self-diffusion coefficient of liquid water. These quantities, although important, are primitive descriptors of the fluid, and even so, comparisons amongst available results have been inconsistent. Different groups appear to use somewhat different analysis procedures, not always documented, and even among groups using the same procedure there are quantitative differences in $g_{OO}(r)$'s, the oxygen-oxygen radial distribution. Izvekov and Voth [4] noted this point and helpfully explored the relevant details that went into their calculation of the $g_{OO}(r)$ and oxygen mean-squared displacement. Quantitative comparisons of properties such as self-diffusion coefficients could be more instructive.

We are unaware of a previous attempt to obtain an entropic thermodynamic property such as the chemical potential on the basis of information from AIMD simulations on water. This is ironic because the unusual beauty of water as a molecular fluid is founded on its peculiar temperature behavior. The phase behavior of water on the surface of the Earth has been well documented; for example, the equilibrium densities of the liquid and vapor phases along the saturation curve are known to a far greater precision than, for instance, the height of the first peak in the $g_{OO}(r)$. Chemical potentials (Gibbs free energies per mole for a one-component system) provide a more basic description of that phase equilibrium. These free energies are interesting in their own right, as a characterization of the molecular interactions, and they play a critical role in aqueous phase chemical reactions. The obvious reason that they have not been evaluated from AIMD work before is that they are less trivial to calculate. An important motivation of the present work is that molecular theory, the quasichemical approach, has progressed to the

state that sensible estimates of chemical potentials can now be obtained from AIMD calculations.

In this paper, we calculate the Gibbs free energy of water on the basis of AIMD simulations. To the best of our knowledge, this is the first such attempt. To achieve this, we interpret the results of the AIMD simulation within the framework of the statistical mechanical quasichemical theory of solutions. We first sketch this theory and then discuss its applications to the present case.

II. QUASICHEMICAL THEORY

The quasichemical theory is founded on describing the solute-solvent interaction by partitioning the system into an inner-sphere region and an outer-sphere region [1,2]. This partitioning permits treatment of the chemically important interactions within the inner sphere in detail while exploiting a simpler model to describe the interaction of inner-sphere material with the rest of the system. A variational check is available to confirm the appropriateness of the partitioning [7], and we will reconsider this point below on the basis of the present data.

Consider a distinguished water molecule, and define an inner sphere or bonding region or observation volume proximal to that chosen water molecule. Here that bonding region is defined simply as a ball centered on the oxygen atom of the H₂O molecule, and different values of the radius of the ball will be considered. The quasichemical rule to calculate the excess chemical potential, the hydration free energy, of the distinguished molecule can be written as

$$\mu^{ex} = RT \ln x_0 - RT \ln \langle \langle e^{-\Delta U/RT} \chi \rangle \rangle_0. \quad (1)$$

Here χ is the indicator function for the event that the inner-shell region is unoccupied. The second term of this equation is the outer-sphere contribution to the excess chemical potential. $\langle \langle \dots \rangle \rangle_0$ is the decoupled averaging associated with the potential distribution theorem [2]. Thus the outer-sphere contribution would provide the hydration free energy for the case that the interactions of the distinguished molecule were altered to prohibit any occupancy of the defined inner shell by any solvent molecule.

The review [2] delves deeper into various aspects of the quasichemical theory, but here we provide a short physical description. In evaluating the chemical potential of the distinguished solute, we can partition the interaction of the solute with the system into a near-field contribution and a far-field contribution. This partitioning is achieved by defining an observation volume surrounding the solute and then using an indicator function. The near-field term, the inner-shell contribution, attempts to capture the chemically important interactions, whereas the outer-sphere contribution captures the packing and far-field effects. The quasichemical rule, Eq. (1), codifies this partitioning.

The probability that the observation volume centered on a distinguished water molecule has n occupants is x_n . x_0 corresponds to the case that this observation volume is empty. The interactions of the distinguished water molecule with the rest of the solution are fully involved. In contrast, the outer-sphere contribution would provide the excess chemical potential

(hydration free energy) for the defined case that the distinguished water molecule was forbidden inner-shell partners. We will estimate that contribution on the basis of a van der Waals model: a cavity free energy $-RT \ln p_0$ plus mean-field estimates of contributions from longer-ranged interactions. Our strategy here is to estimate x_0 and p_0 from the AIMD results and then to model the remaining outer-sphere effects, using distinct but generally available information.

For a given choice of the observation volume, direct observation of x_0 from AIMD simulation would be ambitious. Less ambitious is to infer x_0 from AIMD simulation results for moments that constrain the distribution x_n . Robust estimates of the moments $\langle n \rangle$ and $\langle n^2 \rangle$ can be obtained from AIMD simulations. Utilizing a default distribution $\{\hat{x}_n\}$, we then consider a model incorporating Lagrange multipliers λ_j ,

$$-\ln \left[\frac{x_n}{\hat{x}_n} \right] \approx \lambda_0 + \lambda_1 n + \lambda_2 n^2 \quad (2)$$

in which λ_j are adjusted to conform to the constraints of the available moments. Such an information theory procedure has been used before to model hydrophobic hydration [10,11] and also the case of Na⁺ hydration [7].

Determination of the Lagrange multipliers might be accomplished by a Newton-Raphson procedure (for instance, Ref. [12]). Alternatively, the solution can be obtained by minimizing

$$f(\lambda_1, \lambda_2) = \ln \left[\sum_{n \geq 0} \hat{x}_n e^{-\lambda_1 n - \lambda_2 n^2} \right] + \lambda_1 \langle n \rangle + \lambda_2 \langle n^2 \rangle, \quad (3)$$

with

$$\lambda_0 = \ln \left[\sum_{n \geq 0} \hat{x}_n e^{-\lambda_1 n - \lambda_2 n^2} \right], \quad (4)$$

so that

$$\ln x_0 = - \ln \left[\sum_{n \geq 0} \frac{\hat{x}_n}{x_0} e^{-\lambda_1 n - \lambda_2 n^2} \right]. \quad (5)$$

Operationally, we find that Eq. (3) leads to a rapid solution. [This point was made before [12], but note also the obvious typographical error in Eq. (19) there.]

The outer-sphere contributions will be partitioned into packing effects, electrostatic, and dispersion interactions. For a defined observation volume of radius R , the packing contribution was obtained as follows. Ten thousand points were placed randomly in the simulation box per configuration, and the population of water molecules in the defined volume calculated. These give the quantities p_n . p_0 was then readily obtained by the information theory procedure. $-kT \ln p_0$ directly gives the packing contribution. [This is readily seen from Eq. (1); see also Eq. (1) in Ref. [13].]

The electrostatic effects were modeled with a dielectric continuum approach [14], using a spherical cavity of radius R . The SPC/E [15] charge set was used for the water mol-

ecule in the center of the cavity. For the dispersion contribution, we assume that the solute-solvent (outside the observation volume) interaction is of the form C/r^6 and that the distribution of water outside the observation volume is uniform. Thus the dispersion contribution is $-4\pi\rho C/(3R^3)$, where for the SPC/E water model, $4\pi\rho C/3$ is 87.3 kcal/mole \AA^3 .

III. SIMULATION METHODOLOGY

The AIMD simulations were carried out with the VASP [16,17] simulation program using a generalized gradient approximation, PW91, [18,19] to the electron density functional theory. The core-valence interactions were described using the projector augmented-wave (PAW) method [20,21]. The system is 32 water molecules contained in a cubic box of length 9.8656 \AA . The 32 molecule system was extracted from a well-equilibrated classical molecular dynamics simulation of SPC/E [15] water molecules. This was further energy minimized and then equilibrated (at 300 K) by periodic velocity scaling using the SPC/E potential for more than 20 ps. The hydrogen atoms were replaced by deuterium atoms in the *ab initio* simulation; hence our *ab initio* simulation corresponds to *classical* statistical mechanics of D_2O .

The system obtained classically was first quenched. After a short (less than a picosecond) velocity scaling run, we removed the thermostat. At this stage the input temperature was about 328 K. This system was equilibrated in the NVE ensemble for 10.4 ps. The production run comprised a further 4.4 ps of NVE simulation. This run will be referred to as PW91, corresponding to the functional used. The mean temperature in the production phase was 334 ± 22 K. A 1 fs time step was used for integrating the equations of motions. For the electronic structure calculation, convergence was accepted when the energy difference between successive self-consistent iterations fell below 10^{-6} eV. (The default, and usually recommended, convergence in VASP is 10^{-4} eV.)

From the terminal state of the PW91 run, two separate runs were initiated. One employed the PBE [22] functional and a time step of 0.5 fs. The other simulation employed the revised PBE functional [23] and a time step of 1.0 fs. The PBE run lasted about 6.3 ps, of which the last 3.6 ps comprised the production phase. The rPBE run lasted 7.6 ps of which the last 3.4 ps comprised the production phase. The mean temperature in the PBE run was 337 ± 21 K, and for the rPBE run it was 314 ± 21 K.

IV. RESULTS AND DISCUSSION

A. Structure and dynamics

Figure 1 shows the density distribution obtained in this study. Also shown is the experimental result by Hura and Head-Gordon [24]. The first shell around the distinguished water has about 4.2 (for rPBE) water molecules. This contrasts with classical water models where typically between 4 and 6 water molecules are found in the first shell. In comparison to the experiments, both the PW91 and PBE simulations indicate structuring of the fluid, whereas the rPBE simulation predicts a less structured fluid. (Note also the dif-

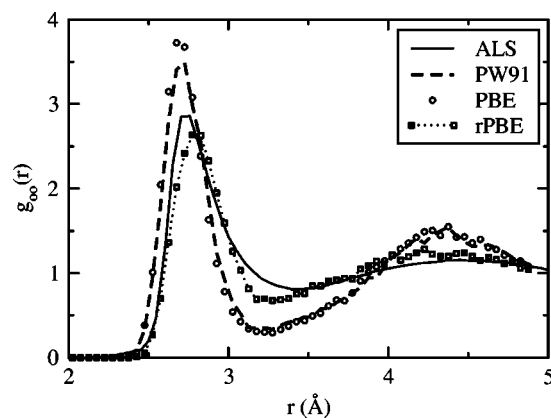


FIG. 1. Oxygen-oxygen radial density distribution. The data were collected in bins of width 0.05 \AA . The current best experimental study using the Advanced Light Source [24] experiment (ALS) is also shown. The PW91 run is at a temperature of 334 K, the PBE run is at a temperature of 337 K, and the rPBE run is at a temperature of 314 K. The experiments are at 300 K.

ferences in temperature between the experiments and the simulations). Nuclear quantum effects will likely soften the computed structures as was suggested by Kuharski and Rossky [25].

To estimate the effect of time step, we further propagated the rPBE run for another 4.4 ps with a time step of 0.5 ps. Initial velocities were assigned to give a temperature of 300 K. The mean temperature in the last 1.5 ps of this run was 298 ± 20 K. The $g_{OO}(r)$ for this run is indistinguishable from the $g_{OO}(r)$ for rPBE shown in Fig. 1. Although we expect the $g_{OO}(r)$ to be a bit more structured, the uncertainty in the temperature is large enough, a consequence of small sample size, that it is not surprising that the structures are very similar (within the statistical uncertainties). (Note that for a classical model using two temperatures differing by 20 K and involving a long simulation time does indicate a softening of the structure at higher temperatures, as expected.)

Comparison with other *ab initio* simulations of liquid water serves to benchmark those results. In Table I we collect results on the radial density distribution and diffusion coefficient of several earlier studies. The prevailing nonuniform agreement of simulations results is apparent. A graphical comparison of the density distribution using solely the BLYP functional is provided in Fig. 2, which again emphasizes the nonuniform agreement in earlier simulations using the same methodology.

The deep first minima in the $g_{OO}(r)$ seen in some of our simulations is similar to those seen in the more modern simulations studies in Ref. [28] (Fig. 2) and Ref. [5]. Beyond this the comparison is very nonuniform as illustrated by Fig. 2 and Table I. As noted by Izvekov and Voth [4] one reason for the discrepancy is likely the different analysis procedures used, not all of which have been documented. It is also plausible that different thermostating procedures, especially those involving electronic degrees of freedom in CPMD, could play a role in the observed discrepancies.

A further point suggested by Fig. 2 and Table I is the need to evaluate the sensitivity of the results from Car-Parrinello

TABLE I. Comparison of selected earlier *ab initio* molecular dynamics simulation on water. CP refers to Car-Parrinello dynamics. BO refers to Born-Oppenheimer dynamics. μ is the fictitious mass parameter in CP dynamics. A03 is this work. ISO, NVT, and NVE refer to isokinetic temperature control, canonical ensemble (with Nose-Hoover thermostats, for example), and microcanonical ensemble, respectively. t_{eq} , equilibration time. t_{prod} , production time. T , temperature. g_{max} , height of first peak in $g_{OO}(r)$. DF, density functional. B/LDA, Becke exchange plus local density approximation. BLYP, Becke exchange plus Lee-Yang-Parr correlation functional. PP, pseudopotential, where V is Vanderbilt's ultrasoft pseudopotential, TM is Troulier-Martins pseudopotential, and PAW is projector augmented wave. D , diffusion coefficient. N , the number of water molecules used. NA, not applicable. Where the value of a particular column is not absolutely clear from the citation or was not reported, we have left it blank. The interested reader should consult the primary reference for further details.

Reference	Dynamics	μ (a.u.)	DF	PP	Equilibration	N	t_{eq} (ps)	Production	t_{prod} (ps)	T (K)	g_{max}	D ($\text{\AA}^2/\text{ps}$)
P93 [26]	CP	1100	B/LDA	V		32	1.5		2		2.2	
P96 [27]	CP	1100	BLYP	TM	ISO	32	1.0	NVE	5	300	2.4	0.1
P99 [3]	CP	900	BLYP	TM	ISO	64		NVE	10	318	2.4	0.3
P02 [28]	CP	600	BLYP	TM	NVT	64	2.0		10		3.1	
V02 [4]	CP	1100	BLYP	TM	NVE	64	2.0	NVE	11	307	2.7	0.2
S01 [5]	BO	NA	PW91	V	NVE	32	1.0	NVE	3.5	307	3.0	0.1
A03	BO	NA	PW91	PAW	NVE	32	10.4	NVE	4.4	334 ± 21	3.5 ± 0.3	0.1
A03	BO	NA	PBE	PAW	NVE	32	2.7	NVE	3.6	337 ± 21	3.7 ± 0.1	0.1
A03	BO	NA	rPBE	PAW	NVE	32	4.2	NVE	3.4	314 ± 20	2.6 ± 0.2	0.2

molecular dynamics (CPMD) simulations to the choice of μ . Indeed, Tangney and Scandolo [29] have emphasized “the necessity for checking the dependence of results of CP simulations on the value of the fictitious mass parameter μ .” Those researchers proved that “the fictitious inertia also causes the slow component of the electronic dynamics to exchange momentum and energy with the ions, yielding a departure of the CP forces on the ions from the BO ones for large values of μ .” In other words, a large μ leads to a bias in the force from the Hellmann-Feynman force. A similar conclusion was also independently reached by Iyengar *et al.* [30]. They showed that for mass values as low as 364 a.u. a systematic bias results. They obtained stable dynamics for

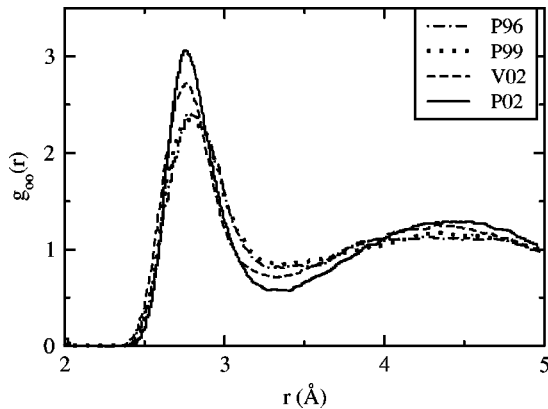


FIG. 2. Oxygen-oxygen radial density distribution obtained by different groups using the BLYP functional and the Car-Parrinello molecular dynamics algorithm. The legend follows the same code as in Table I, which also lists the stated simulation temperature. Except for P96 which was a 32 molecule simulation, all the results are for a 64 molecule simulation.

mass values around 182 a.u. in their studies [30]. Recently, Galli and co-workers [35] have investigated the role of this parameter in NVE simulations of water. Consistent with the present study, they have found enhanced structuring using

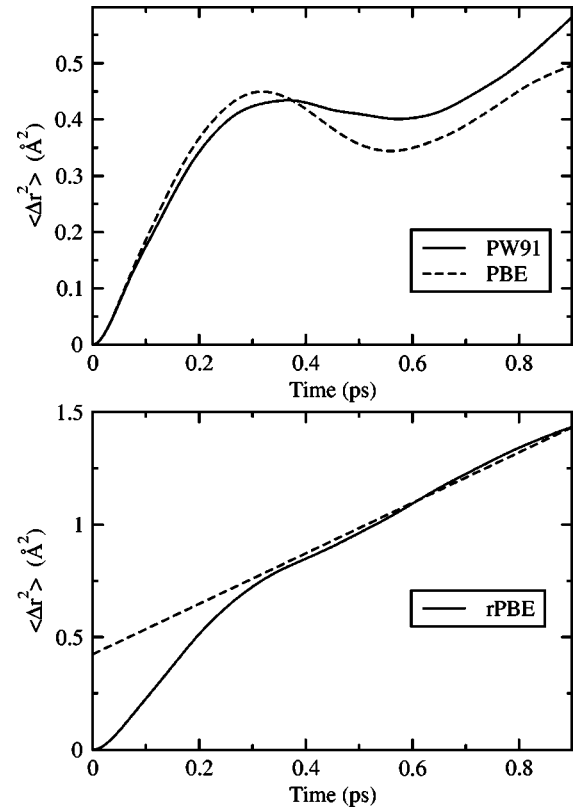


FIG. 3. Mean-squared displacement of oxygen atoms for the various runs. Squared displacements were computed by shifting the time origin by 10 fs prior to averaging. In the bottom panel, the dotted line is the straight line fit to the linear diffusive regime.

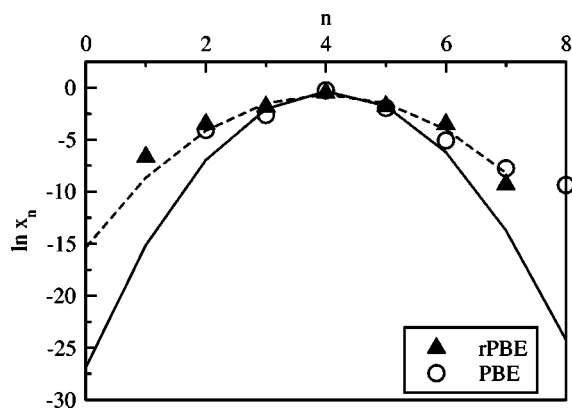


FIG. 4. $\{x_n\}$ vs n . The filled triangles are the rPBE simulation results. The open circles are the PBE results. The dashed line is the information theory (IT) fit to the rPBE results and the solid line is the fit to the PBE results. The Gibbs default distribution, $\hat{x}_j \propto 1/j!$, is used in the IT fits.

the PBE functional, provided a low electron mass parameter is used in CPMD. Using a high value (greater than 800 a.u.) appears to soften the structure.

As indicated in the Introduction, a matter of concern in AIMD simulations is whether these simulation results are glassy compared to water in its liquid phase. Figure 3 shows the mean-square displacement of the oxygen atoms. After a transient of about 0.5 ps, purely diffusive behavior is suggested especially clearly for the rPBE simulation. For the PW91 simulation one can still extract a “diffusion” coefficient from the linear regime, but its value is less clear. Corresponding to the slight structuring of the PBE simulation over the PW91 simulation, a diffusive behavior is less apparent.

The computed diffusion coefficient is $0.2 \text{ \AA}^2/\text{ps}$ at 314 K for the rPBE run. D_2O experimental results are available for various temperatures between 274 K and 318 K [31], based on which we estimate a diffusion coefficient of $0.27 \text{ \AA}^2/\text{ps}$ at 314. Including nuclear quantum effects is expected to increase the calculated diffusion coefficient. Our calculated diffusion coefficient is reasonable, considering the fact that we have only limited statistics. Feller *et al.* [32] have suggested much longer simulation times to obtain statistically satisfying diffusion coefficients.

From Figs. 1 and 3, the PW91 simulation has less fluidity than the rPBE run. The PBE run is even less fluid than the rPBE run. It does appear that the PBE simulation (and possibly the PW91 run) is leading to glassy dynamics at around 330 K.

B. Water hydration free energy

Quasichemical theory provides a framework to compute the hydration free energy from AIMD simulations (Sec. II). The results below are for the rPBE run, unless otherwise noted. We compute $\{x_n\}$ for various radii of the observation volume. The first minima of $g_{\text{OO}}(r)$ is around 3.3 \AA (Fig. 1) and this suggests an inner-sphere radius. In Fig. 4 the $\{x_n\}$ distribution is shown for this particular case. As already mentioned, the wings of the distribution are difficult to ac-

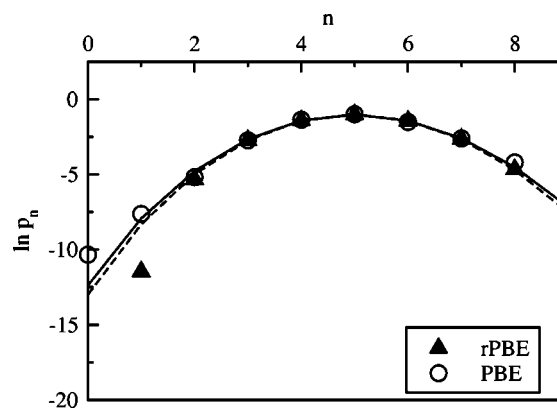


FIG. 5. $\{p_n\}$ vs n . The filled triangles are the rPBE simulation results. The open circles are the PBE results. Rest as in Fig. 4.

cess; in fact only seven distinct occupancies are observed. But the mean and the second moment seem reliable, the maxent model, Eq. (2) is consistent with the direct observations, and thus the model is probably more sensible as a proposed distribution than the direct observations solely. The distribution $\{p_n\}$ for a cavity of size 3.3 \AA is shown in Fig. 5.

A similar procedure can be carried out for observation volumes of different sizes. Of particular interest to us are the sizes $3.0\text{--}3.4 \text{ \AA}$ that bracket the minima in the $g_{\text{OO}}(r)$ (Fig. 1). Figure 6 shows the hydration free energy for cavity sizes in this regime. Here the electrostatic plus dispersion contribution to the outer-sphere term is obtained using the simplified model discussed in Sec. II. In Fig. 6 the minimum for μ^{ex} is obtained for $R=3.3 \text{ \AA}$. This is consistent with the expectations from the $g_{\text{OO}}(r)$ (Fig. 1). It has been argued before [7] that an optimal inner-sphere definition can be identified by the insensitivity of the net free energy to the variations of the inner-sphere region. This is based upon the idea that in the absence of further approximations that net free energy should be independent of the definition of inner sphere. When insensitivity is observed despite inevitable approximations it is possible for those approximations to be jointly satisfactory. Figure 6 confirms this point.

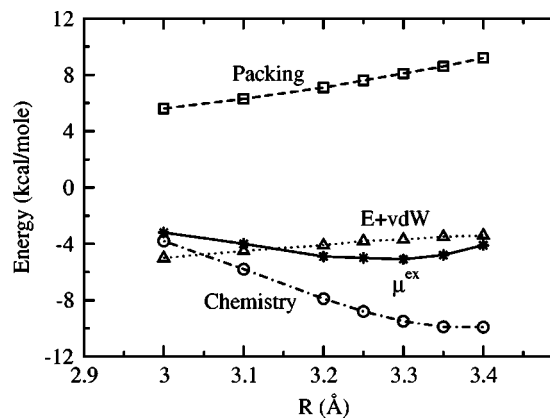


FIG. 6. Cluster variation of the hydration free energy of water. The open circles give the chemical contribution, $RT \ln x_0$. The open squares give the packing contribution, $-RT \ln p_0$. The open triangles give the sum of outer-sphere electrostatic and dispersion contributions. The net free energy is shown by solid line.

Using the values for x_0 and p_0 for a cavity of size 3.3 Å, the sum of the chemical (-9.5 kcal/mole) and packing contributions (8.1 kcal/mole) is -1.4 kcal/mole. From scaled particle theory [33], at 314 K and under saturation conditions, a value of around 6 kcal/mole is expected for the packing contribution. Our computed value is a bit higher because the density is a bit higher than that corresponding to saturation conditions at 314 K. Likewise our chemical contribution is expected to be a bit lower (more negative) than that expected at 314 K under saturation conditions. But since these effects go in opposite directions, they tend to balance out.

For a classical water model, Paliwal and Paulaitis [36] have computed the sum of chemical and packing effects without recourse to the information theory (IT) approach, but relying on about 7 ns of simulation instead. Our IT fits to their data (Asthagiri *et al.*, unpublished observation) yield $-kT \ln x_0$ within 0.5 kcal/mole of their simulated value. The IT estimates of x_0 were found to be insensitive to the choice of either the flat or the Gibbs prior. For a cavity of size 3.4 Å, Paliwal and Paulaitis obtain -0.9 kcal/mole for the chemical (-7.8 kcal/mole) plus packing (6.9 kcal/mole) effect, whereas we obtain -0.7 kcal/mole for the same sized cavity. As indicated above, our chemical contributions are somewhat more negative (Fig. 6) and the packing contributions are somewhat more positive (Fig. 6) than the values obtained by Paliwal and Paulaitis. The distinguishing aspect here is *not* in agreement for the net sum, especially considering our slightly higher temperature (and hence a higher density) than their simulations at 298 K. The distinguishing aspect here is *the inner-sphere chemical effects very nearly balance the outer-sphere packing effects.*

For the outer-sphere electrostatic and dispersion contribution, Paliwal and Paulaitis have explicitly evaluated the second term of Eq. 1 using their classical model. Their computed sum is about 2.5 kcal/mole more negative than that obtained by our simplified model. Thus a more rigorous computation is expected to yield a hydration free energy around -7.5 kcal/mole. In either case, the computed hydration free energy is within 1 kcal/mole of the experimental value.

A similar analysis for the results from the PW91 and PBE functionals gives a hydration free energy of -12.3 kcal/mole and -14.4 kcal/mole, respectively. These are in substantial disagreement with the experimental value. The principal reason is the following. The chemical contributions for the PW91 and PBE runs are -16.5 kcal/mole and -18.2 kcal/mole, respectively. The substantially more negative chemical contribution of -9.5 kcal/mole obtained with the rPBE functional. This is substantially more negative than the -9.5 kcal/mole obtained with the rPBE functional.

In Fig. 4 the distribution from the PBE run is compared with those from the rPBE run. A distinctly non-Gaussian behavior is evident. In this instance the two-moment IT fit is certainly questionable, but we will use it anyway to provide some quantitative comparison with the rPBE results. Note also that x_1 was not obtained, whereas x_8 was (Fig. 4). This suggests a tighter binding with more “empty” pockets in the fluid. This is clearly found in Fig. 5, where unlike the case for rPBE, even with limited statistics, we could calculate a

p_0 from the simulation. The simulated value is also greater than p_0 inferred from the information theory fit; i.e., IT fits suggest a lower probability of opening a cavity in the fluid than is actually found.

Considering the atomization energy of an isolated water molecule provides some insights into why the revised PBE (rPBE) functional better describes liquid water than PW91 or PBE. The experimental value of the atomization energy is 232 kcal/mole [22,23]. The PW91 and PBE functionals predict [22] 235 kcal/mole and 234 kcal/mole, respectively. The rPBE functional predicts [23] 227 kcal/mole. Thus the rPBE functional is substantially weakening the intramolecular bonds in water and this clearly lies at the heart of why this functional softens the $g_{OO}(r)$ of liquid water and why PBE and PW91 sharpen the structure. The same physical effect likely also leads to a drop in the temperature for the rPBE functional. Likewise the BLYP functional yields an atomization energy around 230 kcal/mole. Once again it is the weakening of intramolecular bonds that likely leads to this functional softening the structure of liquid water in comparison to the PW91 and PBE functionals. Note a caveat when comparison between our PW91/PBE results is being made with earlier results with BLYP. The BLYP results were from CPMD simulations, and as already indicated, published results from different groups [3,4,27,28] do not agree between themselves.

The above comparison of functionals also highlights a conundrum in simulating chemistry with AIMD. Perdew and co-workers have noted the “procrustean” [34] feature of rPBE that it weakens the intramolecular bonds in an isolated water molecule. The same situation applies to BLYP. Although this helps describe liquid water better, the penalty one could pay is the poorer description of local chemical effects. This is of immense concern when studying chemical reactions in liquid water in which water itself is a participant. Such a case arises in the study of an excess proton or proton hole [8] in liquid water. Both the PW91 and PBE functionals underestimate the proton affinity of HO^- by 2 kcal/mole, whereas the BLYP functional underestimates this value by about 5 kcal/mole. The rPBE functional is also expected to substantially underestimate this proton affinity. Resolution of this conundrum will have to await a next level of development of electronic density functionals.

V. CONCLUSIONS

In this paper we obtain the hydration free energy of water using *ab initio* molecular dynamics simulation in conjunction with the quasichemical theory of solutions. Our approach requires determination of a coordination number distribution $\{x_n\}$, the fraction of molecules with n inner-shell neighbors. The quantity x_0 , of fundamental significance in the quasichemical theory, is obtained by a maximum entropy approach. The outer-sphere packing contribution was calculated by calculating p_0 , where p_0 is the probability of observing zero water molecules in a defined volume. The quasichemical theory identified an inner-sphere radius of 3.3 Å where the resulting free energy is insensitive to slight adjustments of that inner-sphere region. This is physically consistent with radius of the first minimum in $g_{OO}(r)$. The chemical and packing contributions provide nearly canceling

contributions to the hydration of water, the net sum being -1.4 kcal/mole. Including outer-sphere dispersion and electrostatic effects yields a final value of -5.1 kcal/mole in reasonable agreement with the experimental value of -6.1 kcal/mole at 314 K. An important physical conclusion is that the quasichemical approach [1,2] provides a natural description of the statistical thermodynamics of liquid water. In this analysis, competition between inner-shell chemical contributions and packing contributions associated with the outer-shell term are decisive. Cases in which there is a substantial skew in either quantity lead to estimates of the hydration free energy substantially different from experiments.

ACKNOWLEDGMENTS

We thank H. S. Ashbaugh for his critical reading of the manuscript and helpful discussions. We thank Amit Paliwal and Mike Paulaitis for their helpful comments and for sharing their work on the classical water simulations prior to publication. We thank Guilia Galli and Eric Schwegler at LLNL for discussing their results pertaining to the role of the fictitious mass parameter in CPMD. The work at Los Alamos was supported by the U.S. Department of Energy, Contract No. W-7405-ENG-36, under the LDRD program at Los Alamos.

-
- [1] G. Hummer, S. Garde, A.E. Garcia, and L.R. Pratt, *Chem. Phys.* **258**, 349 (2000).
- [2] M.E. Paulaitis and L.R. Pratt, *Adv. Protein Chem.* **62**, 283 (2002).
- [3] P.L. Silvestrelli and M. Parrinello, *J. Chem. Phys.* **111**, 3572 (1999).
- [4] S. Izvekov and G.A. Voth, *J. Chem. Phys.* **116**, 10 372 (2002).
- [5] P. Vassilev, C. Hartnig, M.T.M. Koper, F. Frechard, and R.A. van Santen, *J. Chem. Phys.* **115**, 9815 (2001).
- [6] S.B. Rempe, L.R. Pratt, G. Hummer, J.D. Kress, R.L. Martin, and T. Redondo, *J. Am. Chem. Soc.* **122**, 966 (2000).
- [7] S.B. Rempe and L.R. Pratt, *Fluid Phase Equilib.* **183-184**, 121 (2001).
- [8] D. Asthagiri, L.R. Pratt, J.D. Kress, and M.A. Gomez, Los Alamos National Laboratory Technical Report LA-UR-02-7006, 2002, <http://www.arxiv.org/abs/physics/0211057>
- [9] D. Asthagiri and L.R. Pratt, *Chem. Phys. Lett.* **371**, 613 (2003).
- [10] G. Hummer, S. Garde, A.E. Garcia, A. Pohorille, and L.R. Pratt, *Proc. Natl. Acad. Sci. U.S.A.* **93**, 8951 (1996).
- [11] L.R. Pratt, *Annu. Rev. Phys. Chem.* **53**, 409 (2002).
- [12] G. Hummer, S. Garde, A.E. Garcia, M.E. Paulaitis, and L.R. Pratt, *J. Phys. Chem. B* **102**, 10 469 (1998).
- [13] L.R. Pratt, R.A. LaViolette, M.A. Gomez, and M.E. Gentile, *J. Phys. Chem. B* **105**, 11 662 (2001).
- [14] B.J. Yoon and A.M. Lenhoff, *J. Comput. Chem.* **11**, 1080 (1990).
- [15] H.J.C. Berendsen, J.R. Grigera, and T.P. Straatsma, *J. Phys. Chem.* **91**, 6269 (1987).
- [16] G. Kresse and J. Hafner, *Phys. Rev. B* **47**, RC558 (1993).
- [17] G. Kresse and J. Furthmüller, *Phys. Rev. B* **54**, 11 169 (1996).
- [18] Y. Wang and J.P. Perdew, *Phys. Rev. B* **44**, 13 298 (1991).
- [19] J.P. Perdew, J.A. Chevary, S.H. Vosko, K.A. Jackson, M.R. Pederson, D.J. Singh, and C. Fiolhais, *Phys. Rev. B* **46**, 6671 (1992).
- [20] P.E. Blöchl, *Phys. Rev. B* **50**, 17 953 (1994).
- [21] G. Kresse and D. Joubert, *Phys. Rev. B* **59**, 1758 (1999).
- [22] J.P. Perdew, K. Burke, and M. Ernzerhof, *Phys. Rev. Lett.* **77**, 3865 (1996).
- [23] Y. Zhang and W. Yang, *Phys. Rev. Lett.* **80**, 890 (1998).
- [24] T. Head-Gordon and G. Hura, *Chem. Rev. (Washington, D.C.)* **102**, 2651 (2002).
- [25] R.A. Kuharski and P.J. Rossky, *J. Chem. Phys.* **82**, 5164 (1985).
- [26] K. Laasonen, M. Sprik, M. Parrinello, and R. Car, *J. Chem. Phys.* **99**, 9081 (1993).
- [27] M. Sprik, J. Hutter, and M. Parrinello, *J. Chem. Phys.* **105**, 1142 (1996).
- [28] B. Chen, I. Ivanov, J.M. Park, M. Parrinello, and M.L. Klein, *J. Phys. Chem. B* **106**, 12 006 (2002).
- [29] P. Tangney and S. Scandolo, *J. Chem. Phys.* **116**, 14 (2002).
- [30] S.S. Iyengar, H.B. Schlegel, J.M. Millam, G.A. Voth, G.E. Scuseria, and M.J. Frisch, *J. Chem. Phys.* **115**, 10 291 (2001).
- [31] R. Mills, *J. Phys. Chem.* **77**, 685 (1973).
- [32] S.E. Feller, R.W. Pastor, A. Rojnuckarin, S. Bogusz, and B.R. Brooks, *J. Phys. Chem.* **100**, 17 011 (1996).
- [33] H.S. Ashbaugh and L.R. Pratt, Los Alamos National Laboratory Technical Report No. LA-UR-03-2144, 2003, <http://www.arxiv.org/abs/physics/0307109>.
- [34] J.P. Perdew, K. Burke, and M. Ernzerhof, *Phys. Rev. Lett.* **80**, 891 (1998).
- [35] G. Galli *et al.* (private communication).
- [36] A. Paliwal and M. Paulaitis (private communication).